X-ray and neutron scattering studies of the structure of strontium vanadate glasses

U. Hoppe, R. Kranold

Rostock University, Department of Physics, Rostock, D-18051, Germany

A. Ghosh

Department of Solid State Physics, Indian Association for the Cultivation of Science, Jadavpur, Calcutta 700 032, India

J. Neuefeind

Hamburger Synchrotronstrahlungslabor HASYLAB am Deutschen Elektronen-synchrotron DESY, Notkestr. 85, D-22607 Hamburg, Germany

D. T. Bowron

ISIS Facility, Rutherford Appleton Laboratory, Chilton, Didcot OX11 0QX, UK

The structure of a series strontium vanadate glasses is studied by x-ray and neutron diffraction experiments. A decrease of the total V–O coordination number from 4·3±0·2 (10 mol% SrO) to 4·0±0·2 (50 mol% SrO) is observed which is interpreted as a transition from networks formed of VO_5 and VO_4 units to structures formed of only VO_4 tetrahedra. The total V–O coordination number seems to be constant up to 30 mol% SrO and it decreases beyond this stoichiometry. The V–O distance peak is highly asymmetric and needs approximation by two or three Gaussian functions. The total Sr–O coordination number is about 8 also with asymmetric Sr–O distance peaks composed by two Gaussian functions. The V–V distances decrease from 0·344 nm (10 mol% SrO) to 0·337 nm in Sr vanadate glasses of 50 mol% SrO.

Interest in vanadate glasses is due to their semiconducting properties which are based on the coexistence of two oxidation states of the V atoms. The hopping of an unpaired $3d^1$ electron from a V^{4+} to a V^{5+} site is the main process for charge transport.[1] Binary vanadate glasses can be prepared with many of the network forming and network modifying oxides[2] where rapid quenching of the melts is often required. The structure of these glasses is little investigated. Main features of their infrared absorption spectra are high frequency bands at about 1000 cm^{-1} which are attributed to vibrations where the terminal V=O bonds are involved.[2] The band at 1020 cm^{-1} known of vitreous (v-)V_2O_5 is not changed when network forming oxides are added. On the other hand, network modifiers cause a decrease of the frequencies which indicates a coordination of terminal oxygen sites with modifier cations. In some cases, two or more high frequency bands exist such as obtained for the SrO–V_2O_5 glasses[2,3] planned for investigation. By ^{51}V NMR[4] it was detected that the structural units forming the metavanadate networks (50 mol% SrO) are VO_4 tetrahedra while fractions of VO_5 groups occur in glasses of smaller SrO content. ^{51}V NMR measurements of v-V_2O_5[5] confirm these tendencies with the result that a mixture of about equal fractions of VO_4 and VO_5 units form the glassy V_2O_5 networks. Our diffraction data and also structural modelling of v-V_2O_5[6–8] agree with this finding where it is shown that the VO_n units are linked mainly by corners.

For clarifying more structural details of the vanadate glasses modified by SrO, x-ray (XRD) and neutron diffraction (ND) experiments are useful. Information of the V–O coordination can be well obtained in the x-ray correlation functions because Sr–O separations are clearly larger than the V–O first neighbour distances. Since for neutrons the scattering of the vanadium atoms is incoherent the neutron data are an interference of only the three partials Sr–Sr, Sr–O and O–O. In our previous studies of Zn vanadate glasses[8] the change of contrast, i.e. XRD and ND, was used to resolve the V–O and Zn–O distances having similar dimensions. Here, the combination of x-ray and neutron data helps to resolve the Sr–O and O–O first neighbour peaks. The high energy photons received from the wiggler beamline of a synchrotron allow a measuring range up to Q_{max}>300 nm^{-1} where Q is the magnitude of the scattering vector with $Q=4\pi/\lambda\sin\theta$ with λ being the radiation wavelength

*This paper was originally presented at the 2001 International Congress on Glass and the peer reviewed version published as *Phys. Chem. Glasses*, 2002, **43C**, 1–5, a volume with limited circulation. The figures have been reworked and equations reset to aid clarity.
DOI: 10.13036/17533562.61.5.Hoppe

and 2θ the scattering angle. Thus, details of the V–O bonds can be resolved.

Experimental

Sample preparation

The samples are the same as used in previous studies of the electric properties.[9,10] Glass samples of compositions x=10, 20, 30, 40 and 50 were prepared from reagent grade $SrCO_3$ and V_2O_5. Below, these samples are labelled with Sr10, Sr20, Sr30, Sr40 and Sr50. 10 g batches were melted in air in alumina crucibles at temperatures in the range 850–1050°C. The melts were quenched either by pressing between brass plates or by pouring onto a twin roller. The mass densities were obtained with 3·03, 3·19, 3·33, 3·44 and 3·47 g/cm^3. Since the V^{4+} fractions of the Sr vanadate glasses under investigation are small with 4–6%[3,9] the stoichiometric formula used in the analysis is $(SrO)_x(V_2O_5)_{1-x}$. The batch compositions are used for the values x.

X-ray scattering

The XRD experiments were performed on the BW5 wiggler beamline at the DORIS III synchrotron (Hamburg/Germany) with an energy of the incident photons of 130 keV (λ=0·00957 nm). The powdered sample material was loaded into silica capillaries of 2·0 mm diameter and with a wall thickness of 0·01 mm. During the measurements the specimens were positioned in a vacuum vessel to suppress the air scattering. Since the scattering angles are small the transmission factors are assumed to be independent of the angle. The angular increment in the step scan mode was 0·05°. In the full 2θ range from 0·7 to 26° an absorber was set in the diffracted beam to avoid counting rates higher than 10^5 s^{-1}. Other scans without absorber range from 10 to 26°. Details of such experiments and the corrections are described elsewhere.[11] The electronic energy window of the solid state Ge detector was chosen to pass the elastic line and the full Compton profile but no fluorescence scattering. The dead time corrections were made with τ=2·4 μs. A fraction of 0·91 of the incident photons is polarised horizontally. Both numbers allow to merge the data of the scans obtained for both absorber settings and with different synchrotron currents. Corrections are made for background, container scattering and absorption. The scattering intensities are normalised to the structure independent scattering functions which have been calculated by polynomial fits of the tabulated atomic parameters of the elastic and Compton scattering data.[12] Finally, the Compton fractions are subtracted and Faber–Ziman structure factors, $S_X(Q)$, are calculated.[13] XRD data of v-V_2O_5 already published[8] are involved in the analysis to to give a more complete view of the changes.

Neutron scattering

ND experiments of the same samples were performed on the time-of-flight instrument SANDALS of the pulsed neutron source ISIS at the Rutherford Appleton Laboratory. The powdered material was loaded into thin walled vanadium cylinders of 5 mm diameter and with a wall thickness of 0·025 mm. Due to limitations of available sample material the beam height was reduced to 1 cm. The absorption and multiple scattering corrections are made by the ATLAS program suite.[14] The self scattering contributions are calculated according to the compositions of the samples where the inelasticity effects are small due to the small scattering angles of SANDALS. The scattered intensities recorded in the various detector groups and normalised to separate self terms are merged to the differential scattering cross section. Due to the small quantities of the samples and the limitations in the measuring time the data beyond 200 nm^{-1} are already very noisy. However, since Sr–O and O–O correlations with broad peaks dominate the neutron data not much information is expected at higher Q. Finally, the incoherent scattering is subtracted and total neutron structure factors, $S_N(Q)$, are calculated.[13] Neutron diffraction measurements are sensitive to water contaminations of the samples because the self scattering of hydrogen is strong (mostly incoherent) with a slope toward the high Q range. Such effects are not observed and thus possible water contaminations are less than 1 mol%. Nevertheless, humidity may play a critical role for the recrystallisation of glassy vanadate samples.

Results

The structure factors $S_X(Q)$ and $S_N(Q)$ of the samples measured are shown in Figures 1 and 2. Due to the

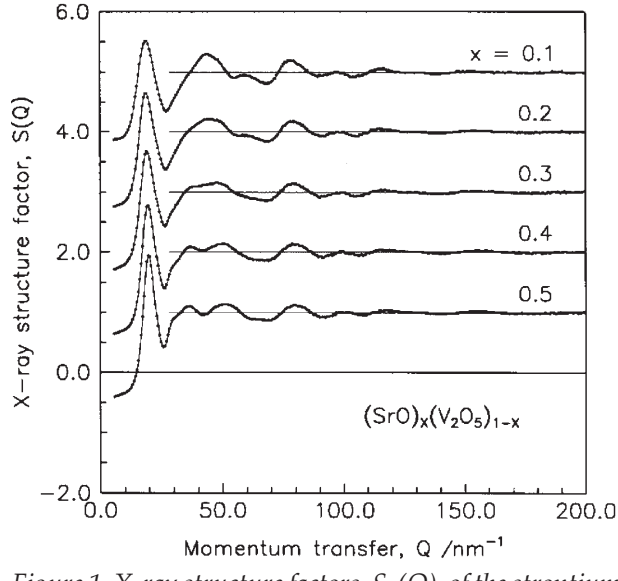

Figure 1. X-ray structure factors, $S_X(Q)$, of the strontium vanadate glasses studied versus the mole fractions, x, of SrO. The upper functions are shifted for clarity

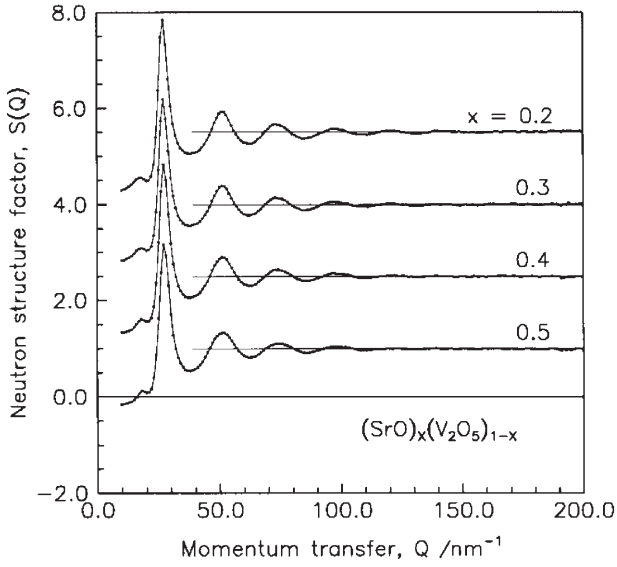

Figure 2. Neutron structure factors, $S_N(Q)$, of four strontium vanadate glasses versus the mole fraction, x, of SrO. The upper functions are shifted for clarity

use of high energy photons the $S_X(Q)$ functions are available up to 280 nm^{-1} but the noisy data beyond 230 nm^{-1} show some unrealistic features and are not used. The changes due to SrO additions which are visible in the $S_X(Q)$ data are small but systematic. On the other hand, the $S_N(Q)$ data are not changed with the SrO additions. The lengths of the O–O edges of the VO_n polyhedra and the Sr–O first neighbour distances whose correlations dominate the scattering of neutrons are nearly equal to each other. Thus, the first main maximum at 28 nm^{-1} in the $S_N(Q)$ data reflects a 'packing' of the large oxygen anions together with Sr^{2+} cations while the invisible V sites fill some specific 'interstices' having no Sr first neighbours. Since the V and Sr atoms are strong scatterers for x-rays the O–O correlations play only a minor role in the XRD data. The first maxima of the $S_N(Q)$'s at ≅28 nm^{-1} are not visible in the $S_X(Q)$ data. Here the first maxima are found at ≅18 nm^{-1}. They are seen as prepeaks in the $S_N(Q)$'s.

The information of the short range order is extracted from the correlation functions, $T(r)$, by peak fitting procedures. The correlation functions are obtained from the $S(Q)$ data by Fourier transformation (FT) with

$$T_k(r)=4\pi r\rho_0+2/\pi\int_0^{Q_{max}} Q[S_k(Q)-1]\sin(Qr)dQ \qquad (1)$$

where ρ_0 is the number density of atoms. No damping is applied in the FT procedure. Parameter k is either X or N for the XRD and ND data. The number densities used are calculated from the mass densities[9] given above. ρ_0=68·8 nm^{-3} is used for v-V_2O_5.[5,6] The resulting $T(r)$ data are compared in Figures 3 and 4 with model functions according to the final fit. The Q_{max}'s used in the FT calculations are indicated in the plots.

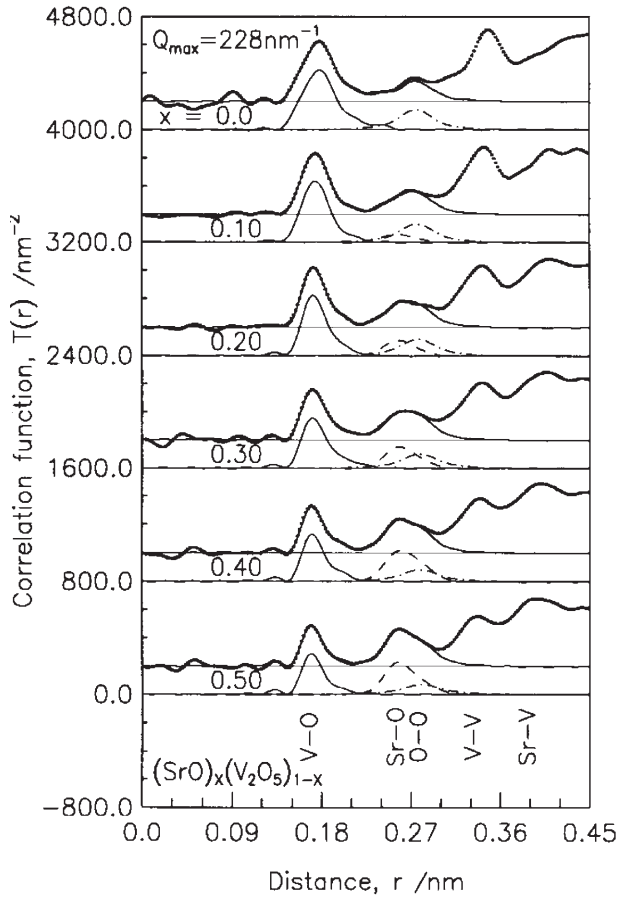

Figure 3. Experimental x-ray correlation functions, T(r), (dotted lines) in comparison with the model T(r) functions (solid lines) fitting the first neighbour V–O, Sr–O and O–O distances. Partial contributions given are broadened according to the effects of the Fourier transformations with Q_{max}=228 nm^{-1}: V–O (thin solid lines), Sr–O (dashed lines), O–O (dash–dotted lines). The upper functions are shifted for clarity. The data of v-V_2O_5 (x=0) are taken from previous work[8]

The $T_X(r)$ functions (cf. Figure 3) show asymmetric V–O peaks at ≅175 nm with a long tail on its right side. The small O–O peak at 0·28 nm for v-V_2O_5 is more and more replaced by a strong and asymmetric Sr–O peak at 0·26 nm. Different from the Zn glass series[8] here the V–V peak at 0·34 nm does not interfere with other strong contributions. The V–V distances shorten with SrO additions. The main feature of the $T_N(r)$ functions (cf. Figure 4) is the O–O peak at 0·28 nm. The Sr–O contribution at 0·26 nm causes only a broadening of this peak. The V–O peak at 0·175 nm is visible as a very small negative contribution. Note, vanadium has a very small but negative coherent scattering length.

Parameters of the V–O, Sr–O and O–O first neighbour peaks are extracted by Gaussian fitting. The effects of the truncation at Q_{max} of the $S(Q)$ data used in the FT calculations are taken into account by a method described elsewhere[15] where in the case of the x-ray data also the Q dependent weighting factors are introduced. For fitting the $T(r)$ data the Marquardt

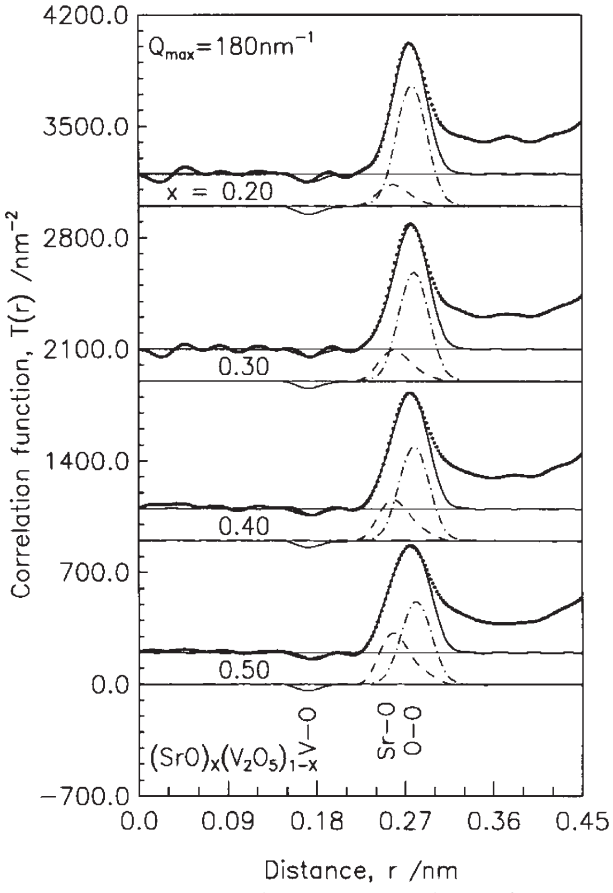

Figure 4. Experimental neutron correlation functions, T(r), (dotted lines) in comparison with the model T(r) functions (solid lines) fitting the first neighbour V–O, Sr–O and O–O distances. Partial contributions given are broadened according to the effects of the Fourier transformations with Q_{max}=180 nm^{-1}: V–O (thin solid lines), Sr–O (dashed lines), O–O (dash–dotted lines). The upper functions are shifted for clarity

Table 1. Parameters resulting from the Gaussian fits of first neighbour distances which are simultaneously performed in the x-ray and neutron correlation functions, $T_X(r)$ and $T_N(r)$, such as shown in Figures 3 and 4. For the Sr10 sample only $T_X(r)$ data are fitted and thus the corresponding parameters are somewhat arbitrary. The parameters of v-V_2O_5 are little changed if compared with those published previously[8]

Sample	*Atom pair*	*Coordination number*	*Distance (nm)*	*FWHM (nm)*
v-V_2O_5	V–O	1·40	0·1630	0·019
		2·10	0·1820	0·019
		0·90	0·2020	0·022
		0·40	0·2320	0·030
	O–O	6·00(15)	0·2750(20)	0·035(4)
Sr10	V–O	1·35	0·1630	0·017
		2·45	0·1790	0·020
		0·50	0·1990	0·023
	Sr–O	5·80	0·2520	0·030
		3·70	0·2700	0·036
	O–O	6·10(15)	0·2760(20)	0·036(4)
Sr20	V–O	2·00	0·1665	0·018
		1·70	0·1800	0·020
		0·55	0·1980	0·023
	Sr–O	5·40	0·2535	0·030
		3·45	0·2705	0·036
	O–O	6·00(15)	0·2770(20)	0·036(4)
Sr30	V–O	2·00	0·1665	0·017
		1·75	0·1815	0·021
		0·55	0·2050	0·030
	Sr–O	5·30	0·2545	0·030
		3·40	0·2745	0·036
	O–O	5·80(15)	0·2790(20)	0·036(4)
Sr40	V–O	2·00	0·1670	0·016
		1·60	0·1790	0·021
		0·50	0·1950	0·022
	Sr–O	5·25	0·2540	0·030
		3·25	0·2755	0·036
	O–O	5·40(15)	0·2790(20)	0·036(4)
Sr50	V–O	2·45	0·1675	0·016
		1·50	0·1820	0·022
	Sr–O	5·20	0·2550	0·029
		2·80	0·2780	0·036
	O–O	5·20(15)	0·2810(20)	0·036(4)

algorithm[16] is used where coordination numbers, mean distances and full widths at half maximum (FWHM) are the parameters of the model Gaussian functions. The fit for the Sr10 sample is made by hand because a ND experiment was not feasible due to a very limited amount of sample material. The parameters given for v-V_2O_5 are little simplified if compared with those in our previous work.[8] In all other cases (Sr20, Sr30, Sr40, Sr50) the fits of the $T_X(r)$ and $T_N(r)$ data are performed simultaneously.

From previous work it is known[8] that the V–O peak can only be fitted by use of three Gaussian functions. In the case of v-V_2O_5 a fourth broad Gaussian approximates the flat tail. Only for the Sr50 sample the fit was successful using two Gaussians. The fit of the broad peak at 0·27 nm by single Gaussians for the Sr–O and O–O correlations is not successful. Only when two Gaussian functions are used for the Sr–O peak a sufficient quality of the fit results. Thus, highly asymmetric Sr–O first neighbour peaks must be assumed to allow the fit of the x-ray and neutron data at the same time. The O–O peak at 0·28 nm which belongs to the edges of the VO_n polyhedra may also be somewhat asymmetric. However, a possibly existing tail on its right side cannot be extracted due to overlapping with further correlations. The excellent fit of the $T_X(r)$ and $T_N(r)$ data is shown in Figures 3 and 4. All the detailed parameters of the fits are given in Table 1. Except for the limitations for v-V_2O_5 and the Sr10 sample mentioned above also a few parameters of the other samples are not determined independently. The mean distances of the third Gaussians of the V–O correlations are varied arbitrarily. The widths (FWHM) of the second component of the Sr–O peak and of the O–O peak are set equal. The great number of parameters allows to approximate the peaks in the $T(r)$ functions excellently. Since most parameters of the single Gaussian functions have no physical meaning error bars are not given. The various Gaussian functions which are used to approximate asymmetric V–O and Sr–O peaks cannot be attributed to distances of different functionality.

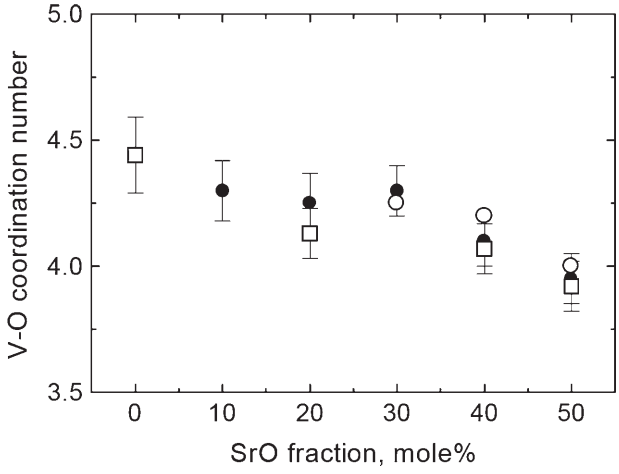

Figure 5. V–O coordination numbers versus SrO fraction (filled circles, this work) in comparison with data obtained by ^{51}V NMR[4] (hollow circles) and our previous data of Zn vanadate glasses[8] (hollow squares)

The total coordination numbers and mean distances of these peaks are given in Table 2. Their uncertainties are estimated and given in this table also (values in parentheses). For v-V_2O_5 also, total numbers of the V–O peak are given which exclude the fourth Gaussian. Distances beyond 0·22 nm exceed lengths of typical V–O bonds and for comparison with the data of the other samples this upper limit of V–O distances is justified.

Discussion

A first clear result of the diffraction investigations of $(SrO)_x(V_2O_5)_{1-x}$ glasses is the change of the total V–O coordination number, N_{VO}, from 4·3 to 4 with SrO additions from 10 to 50 mol%. Thus VO_5 and VO_4 units form the networks of glasses of SrO fractions less than 0·5 while only VO_4 tetrahedra remain in the metavanadate glass. This change is illustrated in Figure 5 where also results of ^{51}V NMR measurements[4] of SrO–V_2O_5 glasses and diffraction results[8] of ZnO–V_2O_5 glasses are shown. In the limits of error all three experiments show the same behaviour of N_{VO}. The new N_{VO} numbers indicate a subtle change near the Sr30 sample. From Sr10 to Sr30 N_{VO} seems to be constant and it decreases beyond Sr30. This discontinuity does not much exceed the uncertainties. Further studies should clarify these small effects.

^{51}V NMR experiments[4] of alkaline earth vanadate glasses have shown that similar effects of modifier additions as known of phosphate glasses[17] exist in the vicinity of the metavanadate stoichiometry. At first, a change from three-fold linked to two-fold linked VO_4 units occurs and only beyond the metavanadate composition the end VO_4 units are formed. A specific structural feature of vanadate glasses of little additions of modifier oxide is the existence of VO_5 units with fractions of up to 30%. Since v-V_2O_5 is hardly

Table 2. Total coordination numbers, N_{ij}, and mean distances, r_{ij}, of the asymmetric V–O and Sr–O first neighbour peaks which are calculated from the parameters given in Table 1. The numbers of v-V_2O_5 given with asterisks denote values which exclude the flat tail of the V–O peak, thus the peak component at 0·232 nm

Sample	*Atom pair*	N_{ij}	r_{ij} *(nm)*
v-V_2O_5	V–O	4·80(20)	0·1840(20)
		4·40(20)*	0·1800(20)*
Sr10	V–O	4·30(20)	0·1765(20)
	Sr–O	9·5(12)	0·259(5)
Sr20	V–O	4·25(20)	0·1760(20)
	Sr–O	8·8(8)	0·260(5)
Sr30	V–O	4·30(20)	0·1775(20)
	Sr–O	8·7(5)	0·262(4)
Sr40	V–O	4·10(20)	0·1750(20)
	Sr–O	8·5(5)	0·262(3)
Sr50	V–O	3·95(20)	0·1730(20)
	Sr–O	8·0(5)	0·263(3)

prepared free of any crystalline fractions its structure is not well defined. According to our previous diffraction studies[6–8] and the ^{51}V NMR results of Nabavi *et al*[5] v-V_2O_5 has about equal fractions of VO_5 and VO_4 units. Edge connected units play only a minor role.[6–8] Due to reasons of charge compensation the V=O bonds are presumably located in the VO_4 units. Starting from this v-V_2O_5 structure modifier additions cause parallel processes of transformations $VO_5 \rightarrow VO_4$ and of simple breakages of V–O–V links. One or other process may predominate in different compositional ranges which would result in discontinuities. The various properties of the modifier cations can have different effects from this behaviour.

Crystal structures which can be related to the glasses studied are known for c-V_2O_5[18] and for c-SrV_2O_6.[19,20] In all these crystal structures the V atoms are five-coordinated with a more distant sixth oxygen nearby. Hence, also distorted VO_6 octahedra can be assumed. Thus a structural conception for explaining the observations made for the glasses cannot be developed on the basis of the related crystals. Only c-BaV_2O_6[21] with chains of corner linked VO_4 units is suggested for comparison with the structure of the Sr50 sample. The mean V–O distance is 0·1715 nm in c-BaV_2O_6[21] which is only little smaller than 0·173 nm observed (cf. Table 2). Different V–O distances to the terminal (O_T) and bridging (O_B) oxygen atoms with lengths of 0·165 and 0·178 nm exist in the crystal which are not resolved in the $T_X(r)$ function of the Sr50 sample (cf. Figure 3). Either the Q_{max} is too small or the fwhm of the V–O_B peak is too large to obtain a split V–O peak.

The V–V distance of the Sr50 glass is about ≅0·337 nm which is smaller than 0·347 and 0·351 nm in c-BaV_2O_6. Thus, chains more entangled exist in the glasses. The V–V distances increase with decreasing SrO fraction and ≅0·348 nm is found for v-V_2O_5.[8] Obviously the increasing number of links and the occurrence of corner linked VO_5 units require greater bridging angles. V–V distances of 0·308 nm known of edge connected VO_5 units in c-V_2O_5[18] can only

play a minor role.

The total Sr–O coordination number varies from 8 to 9 where a first symmetric component of the Sr–O peak lies at 0·254 nm with $N_{SrO} \cong 5{\cdot}5$ (cf. Table 1). N_{SrO} is 9 in the c-SrV_2O_6 structures.[19,20] In Sr metaphosphate glasses $N_{SrO} \cong 6$ was obtained by fitting the Sr–O peak[22] with a single Gaussian. But in subsequent reverse Monte–Carlo simulations,[22] a number N_{SrO} of about 8 with also asymmetric Sr–O peaks was obtained. Irregular polyhedra of 8 to 9 oxygen atoms surround the Sr sites. The more SrO is added the more the Sr share O atoms with neighbouring SrO_n polyhedra. It is the contribution of ionic Sr–O bonds in these polyhedra which leads to the observed increase of the T_g values[9] with increasing SrO fractions. Otherwise, according to the decreasing number of crosslinks in the vanadate networks due to SrO additions one would expect a decrease in T_g.

Conclusions

X-ray diffraction studies of a series of strontium vanadate glasses reveal a decrease of the total V–O coordination number from 4·3±0·2 in 10 mol% SrO to 4·0±0·2 in 50 mol% SrO glasses which agrees with previous observations made by ^{51}V NMR and with diffraction results for a zinc vanadate glass series. The V–O coordination number is nearly constant up to 30 mol% SrO. Beyond this stoichiometry it decreases clearly. The V–O peak is not split into fractions of the shorter bonds with the terminal oxygen sites and the longer bonds with the bridging oxygen sites. However, highly asymmetric distance distributions are observed. The V–V distances decrease from 0·344 nm in 10 mol% SrO to 0·337 nm in 50 mol% SrO glasses. The total Sr–O coordination numbers range from 8 to 9 with asymmetric distance peaks.

Acknowledgements

Financial support of the Deutsche Forschungs–gemeinschaft (contract KR 1372/7-1) is gratefully acknowledged.

References

1. Mott, N. F. *J. Non–Cryst. Solids*, 1968, **1**, 1.
2. Dimitriev, Y., Dimitrov, V., Arnaudov, M. & Topalov, D. *J. Non–Cryst. Solids*, 1983, **57**, 147.
3. Hayakawa, S., Yoko, T. & Sakka, S. *J. Ceram. Soc. Jpn.*, 1994, **102**, 522.
4. Hayakawa, S., Yoko, T. & Sakka, S. *J. Ceram. Soc. Jpn.*, 1994, **102**, 530.
5. Nabavi, M., Sanchez, C. & Livage, J. *Phil. Mag. B*, 1991, **63**, 941.
6. Hoppe, U., Kranold, R. & Gattef, E. *Solid State Commun.*, 1998, **108**, 71.
7. Hoppe, U. & Kranold, R. *Solid State Commun.*, 1999, **109**, 625.
8. Hoppe, U., Kranold, R., Gattef, E., Neuefeind, J. & Keen, D. A. *Z. Naturforsch. A*, 2001, **56**, 478.
9. Sen, S. & Ghosh, A. *J. Phys.: Condens. Matter*, 1999, **11**, 1529.
10. Sen, S. & Ghosh, A. *J. Phys.: Condens. Matter*, 2001, **13**, 1979.
11. Poulsen, H. F., Neuefeind, J., Neumann, H.–B., Schneider, J. R. & Zeidler, M. D. *J. Non–Cryst. Solids*, 1995, **188**, 63.
12. Hubbell, J. H., Veigele, Wm. J., Briggs, E. A., Brown, R. T., Cromer, D. T. & Howerton, R. J. *J. Phys. Chem. Ref. Data*, 1975, **4**, 471.
13. Waseda, Y. In *The structure of non–crystalline materials*. 1980. McGraw–Hill, New York. P 11 ff.
14. Hannon, A. C., Howells, W. S. & Soper, A. C. *IOP Conf. Series*, 1990, **107**, 193.
15. Leadbetter, A. J. & Wright, A. C. *J. Non–Cryst. Solids*, 1972, **7**, 23.
16. Marquardt, D. *SIAM J. on Appl. Math.*, 1963, **11**, 431.
17. Brow, R. K. *J. Non–Cryst. Solids*, 2000, **263&264**, 1 and references therein.
18. Enjalbert, R. & Galy, J. *Acta Crystallogr. C*, 1986, **42**, 1467.
19. Karpov, O. G., Simonov, M. A., Krasnenko, T. I. & Zabara, O. A. *Kristallografiya*, 1989, **34**, 1392.
20. Schnuriger, B., Enjalbert, R., Savariault, J. M. & Galy, J. *J. Solid State Chem.*, 1991, **95**, 397.
21. Yao, T., Oka, Y. & Yamamoto, N. *Inorg. Chim. Acta*, 1995, **238**, 165.
22. Hoppe, U., Walter, G., Kranold, R. & Stachel, D. *J. Non–Cryst. Solids*, 2000, **263&264**, 29.